Overscreening Induced by Ionic Adsorption at the Ionic Liquid/Electrode Interface Detected Using Neutron Reflectometry with a Rational Material Design

AUTHOR(S):

Nishi, Naoya; Uchiyashiki, Junya; Oda, Tatsuro; Hino, Masahiro; Yamada, Norifumi L.

CITATION:

Nishi, Naoya ...[et al]. Overscreening Induced by Ionic Adsorption at the Ionic Liquid/Electrode Interface Detected Using Neutron Reflectometry with a Rational Material Design. Bulletin of the Chemical Society of Japan 2021, 94(12): 2914-2918

ISSUE DATE:

2021-12

URL:

http://hdl.handle.net/2433/274824

Overscreening Induced by Ionic Adsorption at the Ionic Liquid/Electrode Interface Detected Using Neutron Reflectometry with a Rational Material Design

Naoya Nishi,*[1] Junya Uchiyashiki,[1] Tatsuro Oda,[2] Masahiro Hino,[3] and Norifumi L. Yamada[4]

[1]Department of Energy and Hydrocarbon Chemistry, Graduate School of Engineering, Kyoto University, Kyoto 615-8510

[2]Institute for Solid State Physics, University of Tokyo, Kashiwa, Chiba 277-8581

[3]Institute for Integrated Radiation and Nuclear Science, Kyoto University, Kumatori, Osaka 590-0494

[4]Institute of Materials Structure Science, High Energy Accelerator Research Organization (KEK), Ibaraki 305-0801

E-mail: <nishi.naoya.7e@kyoto-u.ac.jp>

Naoya Nishi
Naoya Nishi, Associate Professor at Graduate School of Engineering, Kyoto University, received Ph.D. (2003) of Engineering degrees from Kyoto University. His current research interests include electrochemistry, interfacial spectroscopy, and interfacial chemistry at ionic-liquid interfaces.

Abstract

Neutron reflectometry (NR) has been utilized to study the electric double layer (EDL) of ionic liquids (ILs), however, further improvement of the sensitivity toward interfacial structure would be desirable. We recently proposed two ways to improve the NR sensitivity toward the EDL structure at the IL/electrode interface (*J. Phys. Chem. C*, 123 (2019) 9223). First, as the electrode, a thin film of metal (Nb) was used whose scattering length density (SLD) and thickness were controlled to sensitively analyze the potential dependent EDL structure. Second, the IL cation and anion were chosen so that they have large size and large SLD difference, both of which also increase the sensitivity. In the present study, we have further explored this rational material design for the sensitivity enhancement, by changing the film metal from Nb to Bi whose SLD is closer to those for two bulk materials: Si and the IL used, trihexyltetradecylphosphonium bis(nonafluorobutane sulfonyl)amide. We successfully observed not only the first ionic layer in the EDL but also the overlayers, revealing that the IL cation is specifically adsorbed on the electrode and that the cation-rich first layer induces overscreening in the overlayers up to the third ionic layer.

Keywords: Neutron reflectivity, Specific adsorption, Ionic multilayers

1. Introduction

Ionic liquids (ILs) have been attractive liquid materials for electrochemical applications.[1–5] The electric double layer (EDL) structure of ILs has been investigated by various techniques.[6–10] X-ray reflectometry (XR) is a powerful method that can investigate the interfacial structure at the molecular level because of the characteristics using a beam with a wavelength on the order of angstroms. Since the interference significantly affects the reflectivity, it is possible to investigate not only the first ionic layer on the surface but also overlayers (2nd layer, 3rd layer, etc.). XR has shown that ILs form ionic multilayers at the interface,[11–15] which become alternately charged multilayers when the interface is charged.[16–21] These layering structures reflect the peculiarities of the EDL of ILs: ionic crowding and overscreening.[1,22–25]

Neutron reflectometry (NR) is another attractive technique complementary to XR because it has an element selectivity different from XR. Several NR studies on the structure at the IL/electrode interface have been reported.[26–32] Nevertheless, NR sometimes suffers from low beam fluence and high background compared with XR, which causes narrowing of the measurable q_z range and therefore lowering the resolution (q_z: the momentum transfer along with the surface normal).

We have recently used NR to study the structure at the IL/electrode interface[33] and revealed that a counter ion-rich first layer gradually evolves with increasing the electrode potential. At the highest potential investigated, the first ionic layer was saturated with counter ions because of the ionic-crowding effect. Such gradual evolution of the counter ion-rich layer had not been observed at the electrode interface of ILs, to the best of our knowledge, although at the electrochemical IL/water (W) interface our recent XR study observed gradual evolution of alternately charged ionic bilayers from the overscreening effect.[21]

The achievement was enabled by the sensitivity enhancement of NR to the EDL structure by designing the materials for the electrode and IL. For the electrode, a thin film was used so that multiple fringes in the reflectivity profile can be precisely analyzed well below the q_z upper limit. From the change in the fringe periodicity, the potential dependent EDL structure was successfully extracted. The electrode material was chosen so that the scattering length density (SLD) is close to that of IL and substrate (Si). Noble metals such as Pt and Au are electrochemically stable (inert) but have high SLDs, which reduces the sensitivity to the EDL structure. Rather, we selected Nb as the electrode because of the combination of relatively low SLD and high electrochemical stability. An IL consisting of large-size ions was used because a thicker ionic layer can be more sensitively detected with the

fringe periodicity change. Also, the IL had a large SLD difference between the cation with four alkyl chains and anion with two perfluoroalkyl chains. These material designs allowed us to enhance the sensitivity of the NR reflectivity profile toward the EDL structure and to detect the potential-induced EDL structural change described above.

In the present study, we further advance the above strategy to achieve even higher NR sensitivity to the EDL at the IL/electrode interface. As the electrode material, Bi was used, which has electrochemical stability similar to Nb and has an SLD closer to Si and IL than Nb (2.40 for Bi vs 3.92 for Nb in the unit of 10^{-6} Å^{-2}). As a result, the change in reflectivity profiles became sharper at a lower q_z range than in the Nb case. We were able to observe not only the first ionic layer but also the overlayers in the EDL. The analysis revealed the existence of the specific adsorption of cations on the electrode surface whereby alternately charged overlayers are induced.

2. Experimental

The details of the material preparation and the NR measurements were described elsewhere.[33] Briefly, an IL, [THTDP$^+$][C$_4$C$_4$N$^-$] (see Fig.S2 for the structure), was prepared by mixing [THTDP$^+$]Cl$^-$ (Aldrich) and Li$^+$[C$_4$C$_4$N$^-$] (Mitsubishi Materials), followed by washing the mixture with water to remove the byproduct (LiCl).[12,21] After the purification by column chromatography,[34] [THTDP$^+$][C$_4$C$_4$N$^-$] as a colorless liquid was obtained. As the working electrode, a Bi film was sputter-deposited[35] on a Si substrate with a thickness of 250 Å (see ref 35 for the detail of the ion beam sputter system used). An Al$_4$Ti film on a Si wafer and an Ag foil inserted between PTFE spacers were used as the counter and quasi-reference electrodes, respectively. The potential of the working electrode with respect to the quasi-reference electrode was denoted as E. A constant potential was applied during the NR measurements at either −1.5, 0, +1.5, and +2 V within the polarized potential window (Fig.S3), from at least 10 min before starting the NR measurements, to avoid the effect of ultraslow relaxation of the EDL structure of ILs.[36–38]

The NR measurements were performed by using a horizontal-type neutron reflectometer, SOFIA, at BL16 in J-PARC MLF.[39,40] The data were analyzed using the slab model, where we took into account n slabs between Si and IL: SiO$_2$ native oxide layer, Bi film, and ionic layers in EDL. The number of ionic layers varied from 1 to 4. We call the four models Monolayer, Bilayer, Trilayer, and Tetralayer models. In the n-slab model, the SLD, ρ, as a function of a displacement along the surface normal, z, can be written as

$$\rho(z) = \rho_0 + \sum_{i=1}^{n} (\rho_i - \rho_{i-1}) \left\{ \frac{1 + \mathrm{erf}\left(\frac{z - \sum_{j=1}^{i-1} d_j}{\sqrt{2}\sigma_{i-1,i}} \right)}{2} \right\}$$

where

$$\mathrm{erf}(z) = \frac{2}{\sqrt{\pi}} \int_0^z \exp(-t^2)\, \mathrm{d}t$$

ρ_i and d_i are the SLD and the thickness of the slab i, and $\sigma_{i,i+1}$ is the roughness at the boundary between the slabs i and i+1. The NR data at the four potentials (−1.5, 0, +1.5, and +2 V) were simultaneously fitted using the n-slab model that contains potential-independent common parameters such as those for SiO$_2$ and Bi (Table 1) and potential-dependent parameters for the ionic layers (Table 2). The number of fitting parameters was limited to as small as possible, in order to prevent the overfitting and extract physicochemically meaningful information (see Table S1 for the number of the fitting parameters).

****

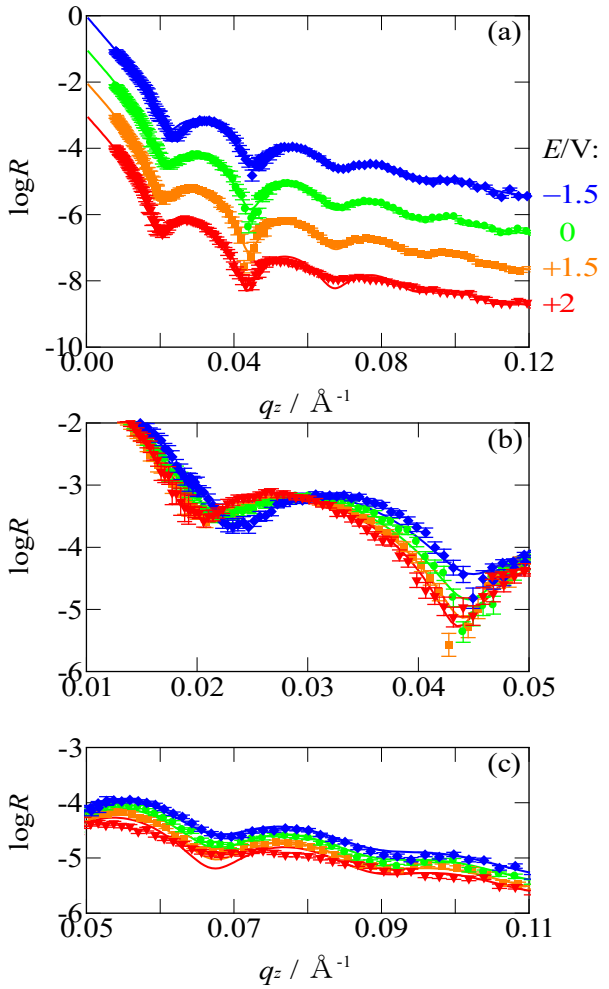

Figure 1. (a-c) Neutron reflectivity profiles (as a function of momentum transfer) at the Si/SiO$_2$/Bi/IL interface at −1.5 (blue diamond), 0 (green circle), +1.5 (orange square), and +2 V (red triangle) in (a) the whole, (b) low, and (c) high q_z regions. The curves are obtained from the fitting with the Trilayer model. Note that the profiles are vertically offset in (a) for clarity but not in (b,c).

****

3. Results and Discussion

Fig.1a shows the logarithmic reflectivity, log$R$, plotted against q_z at four different potentials. The plots clearly show fringes that originate from the Bi layer (and SiO$_2$ layer, see below); the fringe periodicity, 0.023 Å^{-1}, corresponds to 270 Å (=2π/q_z). In Fig.1b shown is the magnified Fig.1a focusing on the potential dependence of the fringe behavior. The fringes exhibit two behaviors for the potential dependence; as going to negative potentials, the fringe periodicity becomes longer and the fringe becomes shallower. These behaviors were also observed in our previous NR study on the EDL at the IL/electrode interface with different IL.[33] The former behavior, i.e., the longer periodicity at more negative potentials, originates from the accumulation of cations, which have low SLD (−0.44 in the unit of 10^{-6} Å^{-2}) compared with the anions

(3.10) and the IL (1.08). The low SLD layer formation due to cation accumulation causes a decrease in the effective thickness of high SLD Bi film in the viewpoint of neutron SLD, leading to longer periodicity. The latter behavior, the shallower fringe dip, also results from the low SLD cationic layer at negative potentials, leading to higher reflectivity with a long periodicity, 0.20 Å^{-1} (corresponding to 32 Å: ionic layer thickness), beyond the observable high q_z region (Fig.1c).[33]

To obtain the information quantitatively, fitting was performed with the four models where the number of ionic layers in the EDL varied from 1 to 4, hereafter called Monolayer, Bilayer, Trilayer, and Tetralayer models. Among the four models, the Monolayer model exhibited a poor fitting result with a relatively high χ^2 value (Table S1). The Bilayer model greatly improved χ^2 and the Trilayer model further did a little. There was no change in χ^2 from the Trilayer model to the Tetralayer model. Generally, the increase in the number of parameters leads to the decrease in χ^2, and therefore we cannot judge the model likelihood from χ^2 when the models we are comparing have a different number of parameters. As a measure of the model likelihood, we used corrected Akaike Information Criterion (AICc).[41] The AICc values were the lowest for the Bilayer and Trilayer models among the four models (Table S1). When the SLD of the third ionic layer in the Trilayer model was set to be potential independent, the AICc became further lower due to a decrease in the number of parameters without a substantial increase in χ^2. These model analyses suggest that the EDL structure, investigated in the present study with the improved detection limit of NR, consists of ionic multilayers up to the third ionic layer. Below in the main text, we discuss the Trilayer model. The fitting results of all the models are shown in Fig.S5.

****

Table 1. Fitting parameters other than those for EDL.

	SLD	Thickness	Roughness
	ρ_i / 10^{-6} Å^{-2}	d_i / Å	$\sigma_{i,i+1}$ / Å
Si	2.07 [a]	-	22.5 [b]
SiO_2	3.54 [a]	22.5	22.5 [b]
Bi	2.49	253.8	8.1 [c]
ionic layer	- [d]	32.3 [e]	8.1 [c]
IL	1.08 [a]	-	-

[a] Fixed. [b] Constrained to be the same value, and equal or less than the thickness of SiO_2 layer. [c] Constrained to be the same value. [d] Potential dependent and see Table 2 for the values. [e] Constrained to be the same value for all the ionic layers.

****

Table 2. Fitting parameters for EDL.

E	SLD (1st layer)	SLD (2nd layer)	SLD (3rd layer)
V	ρ_i / 10^{-6} Å^{-2}	ρ_i / 10^{-6} Å^{-2}	ρ_i / 10^{-6} Å^{-2}
+2	1.08	1.37	1.03 [a]
+1.5	0.97	1.42	1.05 [a]
0	0.75	1.43	1.02 [a]
-1.5	0.45	1.42	1.05 [a]

[a] 1.04 when constrained to be the same (see also Table S1).

****

Table 1 lists the fitting parameters that are potential independent. The SLD for Bi layer was evaluated to be 2.49 (10^{-6} Å^{-2}), which is slightly higher than 2.40 for the bulk Bi, probably due to the partial oxidation of the film. The sum of the thickness for the Bi film and the SiO_2 layer was 276.3 Å, which corresponds to a fringe period of 0.023 Å^{-1} (Fig. 1a and 1b). The thickness of the ionic layer was 32.3 Å, which is in the range of 16-35 Å in our previous NR study.[33]

The potential-dependent fitting parameters are listed in Table 2 and the SLD profile at the Bi/IL interface is shown in Fig. 2 (the overall profile is shown in Fig. S4). The SLDs of the first ionic layer are equal or lower than that of the bulk IL (1.08×10^{-6} Å^{-2}), and they become lower at negative potentials. The SLDs of the cation and anion are −0.44 and 3.10×10^{-6} Å^{-2}, which are lower and higher than that for the IL bulk, respectively. Therefore, the low SLD indicates that the first ionic layer is cation-rich. This agrees with the electrochemical behavior in general; cations are more accumulated on the electrode surface at more negative potentials. On the other hand, even at positive potentials, the SLD did not become higher than that of the IL bulk, i.e., the first ionic layer did not become anion-rich. This would be due to the specific adsorption of cations; non-electric preference of cation on the surface sterically prevent anions from attracted to the surface because ILs have few void.

The second ionic layer was almost independent of the potential, showing high SLDs (Table 2 and Fig.2). In other words, an anion-rich layer was formed. This anion-rich layer is likely to be induced by the cation-rich first ionic layer, which is an overscreening phenomenon in the EDL of ILs.[16,23] The potential independence of the SLD of the second ionic layer would be due to the counterbalance between the induced effect by the cations of the first ionic layer and that by the charge on the electrode surface. The third ionic layer had almost the same as the bulk SLD but slightly lower. This slightly cation-rich layer is also induced by the overscreening effect of the anion-rich second ionic layer.

****

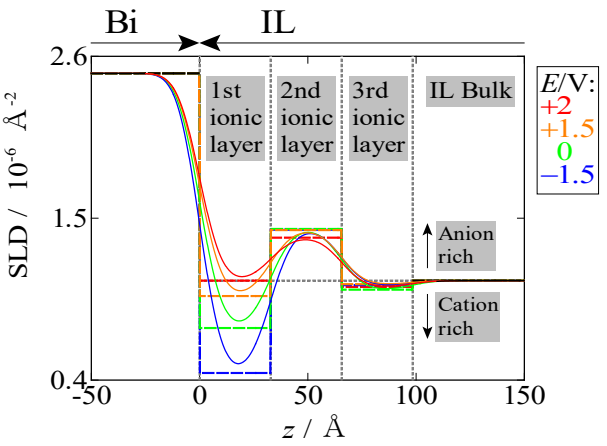

Figure 2. Scattering length density as a function of surface-normal displacement at the Bi/IL interface at −1.5 (blue), 0 (green), +1.5 (orange), and +2 V (red). The vertical gray dotted lines are at the boundaries between ionic layers and horizontal gray dotted line is at the SLD of IL bulk. The dashed lines are hypothetical profiles with zero roughness.

****

The SLD of ith ionic layer (i:1-3) was converted to its contribution to the surface charge density σ_i (see SI for the

derivation). The potential dependence of converted σ_i is shown in Fig. 3. The sum of σ_i corresponds to the surface charge density on the electrode, σ (black). The σ becomes zero around $E = 0$, illustrating that the potential of zero charge (PZC) is around $E = 0$ V. One may think that this is trivial but it is electrochemically not, affected by several factors including the reference electrode, the materials and crystal planes of the electrode, and specific adsorption of ions. From the slope of the plot for σ, the differential capacitance was evaluated to be 7 μF cm^{-2}. This value is almost double the 3.3 μF cm^{-2} by a simple calculation using the Helmholtz model, $\varepsilon_0\varepsilon/(d/2)$ with the dielectric constant $\varepsilon = 6$ for ILs with similar ionic structures[42] and $d = 32$ Å from Table 1 (ε_0: permittivity in vacuum). This increase is rationalized by overscreening[43,44] and specific adsorption,[45] both of which tend to increase the differential capacitance.

****

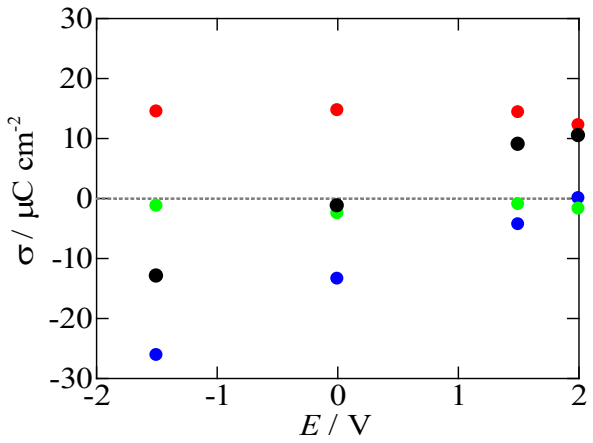

Figure 3. Surface charge density versus potential plots from the Trilayer model fitting results for the 1st layer (blue), 2nd layer (red), 3rd layer (green), and the three layers in total (black).

****

Although the experiments were performed up to at 2 V, within the polarized potential window (Fig.S3), if we were able to make the potential more positive, we would expect the first cation-rich layer to switch to anion-rich (blue, Fig.3). At 2 V, σ_2 starts to decrease (red, Fig.3), and the second anion-rich layer would be replaced with a cation-rich layer at more positive polarization. The third layer is almost neutral. This is consistent with the fact that alternately charged ionic bilayers were observed at the IL/W interface of the same IL.[21] A smaller-size ion would induce multilayers with a greater number, although NR sensitivity will get worse as discussed in Introduction.

The difference in the EDL behavior between Nb in the previous study[33] and Bi in the present study can be due to the difference in the metal; Bi-oxide species such as Bi=O and Bi-OH on the Bi surface may induce the specific adsorption of the cation. Another possibility is the difference in the IL ions ([THTDP$^+$][PFPB$^-$] and [THTDP$^+$][C$_4$C$_4$N$^-$] for the previous and present studies, respectively, where PFPB$^-$ is tetrakis(pentafluorophenyl)borate). One of the characteristics of the IL used in the present study is that the cation is larger than the anion, 833 vs. 624 Å^3. The larger ions would favor the electrode surface entropically, as elucidated by the Asakura-Oosawa theory.[46] On the other hand, no such specific adsorption was observed for the EDL at the IL|W interface of the same IL, [THTDP$^+$][C$_4$C$_4$N$^-$].[21] This is probably because water molecules on the W side of the IL|W interface dislike non-polar moieties of the cation and counterbalances the entropic effect.

A question is, why ionic monolayers were observed in the previous study[33] and ionic bilayers in the present study? One reason would be the higher NR sensitivity to the EDL structure in the present study. Even at the Nb/[THTDP$^+$][PFPB$^-$] interface in the previous study, there may exist the second ionic layer, although it should be hardly visible like the third ionic layer in the present study. Also, anion difference would be the factors. Smaller anion size (624 Å^3 for C$_4$C$_4$N$^-$ compared with 709 Å^3 for PFPB$^-$) indicates that the electrostatic correlation length between ions is longer when normalized with the layer thickness, and therefore the overscreening effect would be stronger. Another factor from anion difference is charge localization in the two anions. The negative charge of C$_4$C$_4$N$^-$ anion is localized around the center N atom whereas PFPB$^-$ anion in the previous study has the negative charge delocalized in the whole structure. Therefore, electrostatic interactions between cation and anion would be stronger for C$_4$C$_4$N$^-$.

4. Conclusion

NR with a material design strategy was allowed to clarify the structure of ionic multilayers at the electrode interface of an IL with high sensitivity. The evolution and gradual development of adsorbed cationic layer on the electrode and concomitant overscreening in the overlayers were clearly observed as a potential-dependent behavior. Systematically scrutinizing the ion-size dependence of the EDL structure by using this methodology would help us disentangle the two IL peculiarities, ionic crowding and overscreening, appearing in the EDL of ILs.

Acknowledgement

This work was partly supported by JSPS KAKENHI (No. 21H02046) and Izumi Science and Technology Foundation (2020-J-071). The neutron reflectivity experiments were performed at the Materials and Life Science Experimental Facility in J-PARC (Proposal Nos. 2013B0104, 2014A0172, and 2015A0054). This work has been carried out in part under the Visiting Researcher Program of Institute for Integrated Radiation and Nuclear Science, Kyoto University.

References

1. M. V. Fedorov, A. A. Kornyshev, *Chem. Rev.* **2014**, *114*, 2978–3036.
2. R. Hayes, G. G. Warr, R. Atkin, *Chem. Rev.* **2015**, *115*, 6357–6426.
3. M. Watanabe, M. L. Thomas, S. Zhang, K. Ueno, T. Yasuda, K. Dokko, *Chem. Rev.* **2017**, *117*, 7190–7239.
4. X. Wang, M. Salari, D. en Jiang, J. Chapman Varela, B. Anasori, D. J. Wesolowski, S. Dai, M. W. Grinstaff, Y. Gogotsi, *Nat. Rev. Mater.* **2020**, *5*, 787–808.
5. D. S. Silvester, R. Jamil, S. Doblinger, Y. Zhang, R. Atkin, H. Li, *J. Phys. Chem. C* **2021**, *125*, 13707–13720.
6. R. Atkin, G. G. Warr, *J. Phys. Chem. C* **2007**, *111*, 5162–5168.
7. S. Baldelli, *Acc. Chem. Res.* **2008**, *41*, 421–431.
8. J. C. Rubim, F. A. Trindade, M. A. Gelesky, R. F. Aroca, J. Dupont, *J. Phys. Chem. C* **2008**, *112*, 19670–19675.

9. W. Zhou, S. Inoue, T. Iwahashi, K. Kanai, K. Seki, T. Miyamae, D. Kim, Y. Katayama, Y. Ouchi, *Electrochem. commun.* **2010**, *12*, 672–675.
10. K. Motobayashi, K. Minami, N. Nishi, T. Sakka, M. Osawa, *J. Phys. Chem. Lett.* **2013**, *4*, 3110–3114.
11. N. Nishi, Y. Yasui, T. Uruga, H. Tanida, T. Yamada, S. I. Nakayama, H. Matsuoka, T. Kakiuchi, *J. Chem. Phys.* **2010**, *132*, 164705.
12. N. Nishi, T. Uruga, H. Tanida, T. Kakiuchi, *Langmuir* **2011**, *27*, 7531–7536.
13. M. Mezger, B. M. Ocko, H. Reichert, M. Deutsch, *Proc. Natl. Acad. Sci. U. S. A.* **2013**, *110*, 3733–3737.
14. N. Nishi, T. Uruga, H. Tanida, *J. Electroanal. Chem.* **2015**, *759*, 129–136.
15. J. Haddad, D. Pontoni, B. M. Murphy, S. Festersen, B. Runge, O. M. Magnussen, H. G. Steinrück, H. Reichert, B. M. Ocko, M. Deutsch, *Proc. Natl. Acad. Sci. U. S. A.* **2018**, *115*, E1100–E1107.
16. M. Mezger, H. Schröder, H. Reichert, S. Schramm, J. S. Okasinski, S. Schöder, V. Honkimäki, M. Deutsch, B. M. Ocko, J. Ralston, M. Rohwerder, M. Stratmann, H. Dosch, *Science (80-.).* **2008**, *322*, 424–428.
17. R. Yamamoto, H. Morisaki, O. Sakata, H. Shimotani, H. Yuan, Y. Iwasa, T. Kimura, Y. Wakabayashi, *Appl. Phys. Lett.* **2012**, *101*, 130–133.
18. A. Uysal, H. Zhou, G. Feng, S. S. Lee, S. Li, P. Fenter, P. T. Cummings, P. F. Fulvio, S. Dai, J. K. McDonough, Y. Gogotsi, *J. Phys. Chem. C* **2014**, *118*, 569–574.
19. M. Chu, M. Miller, T. Douglas, P. Dutta, *J. Phys. Chem. C* **2017**, *121*, 3841–3845.
20. P. Reichert, K. S. Kjær, T. Brandt Van Driel, J. Mars, J. W. Ochsmann, D. Pontoni, M. Deutsch, M. M. Nielsen, M. Mezger, *Faraday Discuss.* **2018**, *206*, 141–157.
21. S. Katakura, K. I. Amano, T. Sakka, W. Bu, B. Lin, M. L. Schlossman, N. Nishi, *J. Phys. Chem. B* **2020**, *124*, 6412–6419.
22. A. A. Kornyshev, *J. Phys. Chem. B* **2007**, *111*, 5545–5557.
23. M. Z. Bazant, B. D. Storey, A. A. Kornyshev, *Phys. Rev. Lett.* **2011**, *106*, 6–9.
24. Z. A. H. Goodwin, G. Feng, A. A. Kornyshev, *Electrochim. Acta* **2017**, *225*, 190–197.
25. J. P. De Souza, Z. A. H. Goodwin, M. McEldrew, A. A. Kornyshev, M. Z. Bazant, *Phys. Rev. Lett.* **2020**, *125*, 116001.
26. Y. Lauw, M. D. Horne, T. Rodopoulos, V. Lockett, B. Akgun, W. A. Hamilton, A. R. J. Nelson, *Langmuir* **2012**, *28*, 7374–7381.
27. L. R. Griffin, K. L. Browning, S. M. Clarke, A. M. Smith, S. Perkin, M. W. A. Skoda, S. E. Norman, *Phys. Chem. Chem. Phys.* **2017**, *19*, 297–304.
28. G. A. Pilkington, K. Harris, E. Bergendal, A. B. Reddy, G. K. Palsson, A. Vorobiev, O. N. Antzutkin, S. Glavatskih, M. W. Rutland, *J. Chem. Phys.* **2018**, *148*, 1–9.
29. K. Akutsu-Suyama, M. Cagnes, K. Tamura, T. Kanaya, T. A. Darwish, *Phys. Chem. Chem. Phys.* **2019**, *21*, 17512–17516.
30. S. Watanabe, G. A. Pilkington, A. Oleshkevych, P. Pedraz, M. Radiom, R. Welbourn, S. Glavatskih, M. W. Rutland, *Phys. Chem. Chem. Phys.* **2020**, *22*, 8450–8460.
31. N. Zec, G. Mangiapia, M. L. Zheludkevich, S. Busch, J. F. Moulin, *Phys. Chem. Chem. Phys.* **2020**, *22*, 12104–12112.
32. G. A. Pilkington, A. Oleshkevych, P. Pedraz, S. Watanabe, M. Radiom, A. B. Reddy, A. Vorobiev, S. Glavatskih, M. W. Rutland, *Phys. Chem. Chem. Phys.* **2020**, *22*, 19162–19171.
33. N. Nishi, J. Uchiyashiki, Y. Ikeda, S. Katakura, T. Oda, M. Hino, N. L. Yamada, *J. Phys. Chem. C* **2019**, *123*, 9223–9230.
34. M. J. Earle, C. M. Gordon, N. V. Plechkova, K. R. Seddon, T. Welton, *Anal. Chem.* **2007**, *79*, 758–764.
35. M. Hino, T. Oda, M. Kitaguchi, N. L. Yamada, S. Tasaki, Y. Kawabata, *Nucl. Instruments Methods Phys. Res. Sect. A Accel. Spectrometers, Detect. Assoc. Equip.* **2015**, *797*, 265–270.
36. S. Makino, Y. Kitazumi, N. Nishi, T. Kakiuchi, *Electrochem. commun.* **2011**, *13*, 1365–1368.
37. N. Nishi, Y. Hirano, T. Motokawa, T. Kakiuchi, *Phys. Chem. Chem. Phys.* **2013**, *15*, 11615–11619.
38. S. Zhang, N. Nishi, T. Sakka, *J. Chem. Phys.* **2020**, *153*, 044707.
39. N. L. Yamada, N. Torikai, K. Mitamura, H. Sagehashi, S. Sato, H. Seto, T. Sugita, S. Goko, M. Furusaka, T. Oda, M. Hino, T. Fujiwara, H. Takahashi, A. Takahara, *Eur. Phys. J. Plus* **2011**, *126*, 1–13.
40. K. Mitamura, N. L. Yamada, H. Sagehashi, N. Torikai, H. Arita, M. Terada, M. Kobayashi, S. Sato, H. Seto, S. Goko, M. Furusaka, T. Oda, M. Hino, H. Jinnai, A. Takahara, *Polym. J.* **2013**, *45*, 100–108.
41. N. Sugiura, *Commun. Stat. - Theory Methods* **1978**, *7*, 13–26.
42. A. Rybinska-Fryca, A. Sosnowska, T. Puzyn, *J. Mol. Liq.* **2018**, *260*, 57–64.
43. G. Feng, J. Huang, B. G. Sumpter, V. Meunier, R. Qiao, *Phys. Chem. Chem. Phys.* **2011**, *13*, 14723–14734.
44. I. V. Voroshylova, H. Ers, V. Koverga, B. Docampo-Álvarez, P. Pikma, V. B. Ivaništšev, M. N. D. S. Cordeiro, *Electrochim. Acta* **2021**, *379*, 138148.
45. L. R. Allen J. Bard, Faulkner, *Electrochemical Methods : Fundamentals and Applications*, 2nd Ed.; Wiley, 2001.
46. S. Asakura, F. Oosawa, *J. Chem. Phys.* **1954**, *22*, 1255–1256.

Graphical Abstract

<Title>
Overscreening Induced by Ionic Adsorption at the Ionic Liquid/Electrode Interface Detected Using Neutron Reflectometry with a Rational Material Design

<Authors' names>
Naoya Nishi, Junya Uchiyashiki, Tatsuro Oda, Masahiro Hino, Norifumi L. Yamada

<Summary>
The interfacial structure of ionic liquid (IL) at the electrode interface has been studied using neutron reflectometry. A rational material design of the electrode metal film and IL enabled us to observe not only the first ionic layer but also the overlayers. A quantitative analysis revealed the existence of specific adsorption of IL cation on the electrode which induces overscreening in the overlayers up to the third ionic layer.

<Diagram>